

Phase-controlled two-wave mixing in a moving grating

YAMING FENG,¹ YUANLIN ZHENG,¹ JIANJUN CAO,¹ CE SHANG,² AND WENJIE WAN^{1,2,*}

¹State Key Laboratory of Advanced Optical Communication Systems and Networks, Department of Physics and Astronomy, Shanghai Jiao Tong University, Shanghai 200240, China

²University of Michigan-Shanghai Jiao Tong University Joint Institute, MOE Key Laboratory for Laser Plasmas and Collaborative Innovation Center of IFSA, Shanghai Jiao Tong University, Shanghai 200240, China

*Corresponding author: wenjie.wan@sjtu.edu.cn

Received 28 August 2015; revised 6 November 2015; accepted 21 November 2015; posted 23 November 2015 (Doc. ID 241247); published 23 December 2015

Two-wave mixing is fundamental to applications in optical signal processing, holographic information, and imaging science. Conventionally, it takes place in a nonlinear medium where self-induced optical grating can effectively couple two optical waves. However, it demands high input power to trigger nonlinearities and is complicated by the phase shift of the optical grating for the given medium. Here, we separate these physical processes by studying near-degenerated two-wave mixing in a moving grating induced independently by an external acoustic optical modulator. Two-wave mixing is observed under Bragg's phase matching condition, which is greatly affected by phase shifting. Moreover, we show that two-wave mixing here is unidirectional due to the propagation of acoustic waves, which may offer new avenues for applications in optical information processing. © 2015 Optical Society of America

OCIS codes: (190.0190) Nonlinear optics; (190.7070) Two-wave mixing; (190.4223) Nonlinear wave mixing; (190.2055) Dynamic gratings; (230.1040) Acousto-optical devices.

<http://dx.doi.org/10.1364/JOSAB.33.000105>

1. INTRODUCTION

Nonlinear wave mixing is of great importance to optical science and technology. It can bridge several optical channels, allowing information exchange and energy transfer in applications such as optical signal processing, holographic information, and imaging science [1–5]. Its simplest form is the mixing between two waves, which conventionally occurs in a nonlinear medium where the index of refraction nonlinearly responds to the incident beams. Consequently, a spatial index variation can be induced inside due to the interference intensity pattern formed by two waves similar to the process of recording a hologram [6]. Such a spatial index variation is usually in the form of a periodic volume grating, which can successively deflect the incident waves: for example, through Bragg scattering [7,8]. In this manner, energy can be efficiently exchanged between the two waves. One representative example of two-wave mixing (TWM) in photorefractive crystals can allow applications such as phase conjugation mirror and holographic information processing [6,9]. Additionally, TWM has laid a foundation for observing relevant but more complicated phenomena, e.g., optical induced lattices, spatial lattice soliton/shock waves, parity-time (PT) symmetry in optics [10–14]. The induced optical grating here is stationary, and the slow response time (~ seconds) of photorefractive crystals limits their practical usages.

On the other hand, TWM in a moving grating is a more interesting and important subject to study because the dynamics of the moving grating complicates the TWM process in terms of phase matching, directionality [15]. For example, stimulated Brillouin scattering (SBS), having many applications in fiber optics and imaging science [16,17], enables the mixing between near-degenerated two waves in a moving grating induced by stimulated generated phonons through electrostriction [18]. Such SBS exhibits a unique feature of nonreciprocal wave scattering due to the phase-matching condition [19], thus allowing unidirectional energy transport. However, it requires relatively high intensities to trigger such nonlinearity and is difficult to control the phase in this self-matched mechanism unless external index modulation is facilitated [20]. Similar phase problems arise in other physical systems; for example, in photorefractive media, the relative phase between the index variation and the intensity interference pattern spontaneously rising from the spatial drift of photoexcited electrons can be controlled externally through direct current (DC) electric fields [1,21]; in quantum wells, an external DC field must be introduced to vary the near-degenerated TWM in a moving grating [22,23]. Hence, the relative phase here plays an important role in determining the TWM's gain strength and directionality, similar

to the phase-controlled nonlinear process [4,5]. It would be better to isolate the generation of grating and control the phase independently in order to lower the high-intensity demand for TWM and precisely regulate TWM through phase, so that TWM can be more easily accessible and controllable in applications such as all-optical near-degenerated wavelength conversion, optical isolation, and optical switching even at low photon levels.

In this paper, we theoretically and experimentally demonstrate the near-degenerated two-wave mixing effect in a moving optical grating inside an acoustic optical modulator (AOM). We realize a near-degenerated TWM scheme under the exact phase matching condition by carefully choosing the incidence at the Bragg angles. By individually controlling the input waves' intensity ratio and phases, we show that the nature of TWM is due to interference, and the relative phase of the two near-degenerated waves is crucial in determining the energy transfer between the two waves. Moreover, such TWM is unidirectional with respect to the propagation of the moving grating. We expect this new TWM scheme will be helpful in nonmagnetic optical power isolations, which do not have strict requirements in optical frequency and offer new avenues for low-light all-optical information processing applications in the near future.

2. PHYSICAL CONCEPT

In the physical process of acoustic-optic Bragg scattering, an incident laser can be scattered off an acoustic-induced moving grating. The scattered wave is frequency-shifted by the amount of the acoustic wave's frequency. Furthermore, the wave's propagation direction is altered under the Bragg scattering condition. During the process, the Bragg condition and phase matching determine the direction of generated phonons, consequently leading to a frequency upshifted or downshifted scattered wave depending on the incidence. Normally, the acoustic wave here is spontaneously generated through the nonlinear electrostrictive effect, which later can be enhanced by stimulated BS. Meanwhile, under the external acoustic field, e.g., in an AOM, Bragg condition induced scattering also can occur linearly (no dependence on the input power), usually with only one input beam. With two or more input beams, the coupling between the beams only happens with the aid of the acoustic-induced grating but is complicated by their phases and frequency differences.

First, we start with a simple and well-known case of TWM in a stationary grating, e.g., TWM in a photorefractive crystal: the two input waves with the same frequency interfere with each other, thus generating a stable intensity pattern. The photorefractive-induced index variation contains the exact same spatial periodicity as the interference pattern but is slightly shifted due to the spatial charge drift [21,22]. Thanks to this finite phase difference between the index variation and the intensity interference pattern, two-wave mixing/amplification is allowed; otherwise, no energy can exchange between the two waves. On the other hand, when two waves are incident into an AOM [Fig. 1(a)], where a moving optical grating is induced by an acoustic wave while the interference pattern of two waves with the same frequency is stationary, any coupling between the two waves in a moving grating will be averaged out, thus eliminating TWM. TWM can take place again only if the

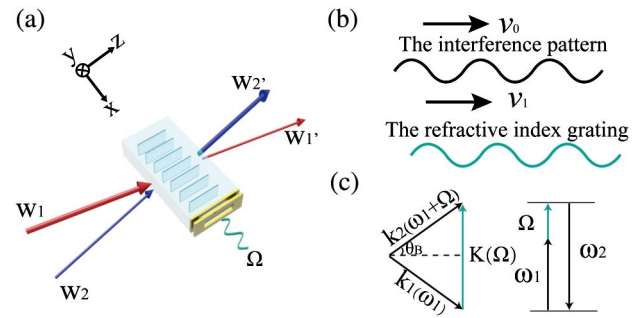


Fig. 1. Two-wave mixing process in a moving grating. (a) Two incident waves (W_1 and W_2) mix in a moving periodic refractive index grating induced by an acoustic wave with frequency Ω into two new waves W_1' and W_2' . (b) Interference pattern (black curve) induced by the two waves has a slight phase shift compared with the refractive index grating (cyan curve), and their periodicities are the same; both conditions ensure the TWM. (c) Phase matching conditions: Conservations of momentum and energy need to be satisfied simultaneously, i.e., $k_2 = k_1 + K$ and $\omega_2 = \omega_1 + \Omega$.

interference pattern moves as well [Fig. 1(b)]. Intuitively, it requires that the moving grating and the interference pattern have the same velocities $v_0 = v_1$ as well as their spatial periodicities. This can be further deduced to fulfill the Bragg scattering condition [Fig. 1(c)] for two near-degenerated waves with finite frequency difference of the moving grating, where their incidences at the first Bragg angles decide the spatial periodicity of the interference pattern matching the moving grating, and their frequency difference equaling to the acoustic wave's ensures that the traveling speeds are the same.

Theoretically, we consider two incident waves E_1 and E_2 with wavelength λ entering into an AOM where the acoustic-induced dielectric tensor is periodically modulated as $\Delta\epsilon(z, t) = \Delta\epsilon \cos(\Omega t + Kx)$, along the transverse $-x$ direction, where $\Delta\epsilon = -\epsilon(pS)\epsilon/\epsilon_0$, ϵ is the dielectric tensor of the acoustic-optical crystal, p is the photoelastic constant, S is the strength of the strain field caused by the acoustic, and ϵ_0 is the dielectric constant of the vacuum. The periodical perturbation of the dielectric tensor can be regarded as a moving grating with velocity v_Ω and period $\Lambda = 2\pi v_\Omega/\Omega$. The incident angles of the two waves have to fulfill the Bragg conditions at the angles of $\pm\theta_B = \lambda/2\Lambda$; only in this case, the momentum conservation $k_2 = k_1 + K$ and the energy conservation $\omega_2 = \omega_1 + \Omega$ can be satisfied simultaneously. By calculating the total electric field with the above periodical perturbation of the dielectric tensor in the Helmholtz equation, two coupling equations of the two waves can be obtained as

$$\frac{dA_1}{dz} = -i\kappa_{12}A_2e^{-i\Delta\phi}, \quad (1)$$

$$\frac{dA_2}{dz} = -i\kappa_{12}^*A_1e^{i\Delta\phi}, \quad (2)$$

where $\kappa_{12} = \omega^2\mu\hat{E}_1^* \cdot \Delta\epsilon\hat{E}_1/2\sqrt{|\beta_1\beta_2|}$ is the coupling coefficient [7]. In our case, $\beta_{1,2} = k_{1,2} \cos \theta_B$, so κ_{12} can be rewritten as $\omega\mu c\hat{E}_1^* \Delta\epsilon\hat{E}_1/(4n \cos \theta_B)$, where $n = 2.2597$ is the refractive index of the acoustic optical crystal (AOC), $A_{1,2}$ are the amplitudes of the two waves, and $\hat{E}_{1,2}$ are unit vectors

describing the polarization states of the two waves. The initial phase difference between the two waves is $\Delta\varphi$. Under the assumption of the slow-varying approximation, Eqs. (1) and (2) can be solved for the steady state solution as

$$A_1(z) = A_1(0)e^{i\Delta\varphi} \cos \kappa z + iA_2(0) \sin \kappa z, \quad (3)$$

$$A_2(z) = A_2(0) \cos \kappa z + iA_1(0)e^{i\Delta\varphi} \sin \kappa z, \quad (4)$$

where κ is the absolute value of the coupling coefficient. $A_{1,2}(0)$ are the initial amplitudes of the two waves. Equations (3) and (4) indicate that the two waves exchange energy along the propagation axis z . This process is affected by two factors: (1) their phase difference $\Delta\varphi$; (2) the initial intensities: I_1 , I_2 . For the former, the intensities of the two output waves I'_1 , I'_2 oscillate sinusoidally with respect to the phase varying but π out of phase to each other for equal-intensity input waves in Fig. 2(a). For unequal-intensity input waves in Fig. 2(b), e.g., $I_1 = 0.25$, $I_2 = 0.75$, both output intensities also oscillate with the varying phase difference, but one of them slightly offsets the other. In both cases, the total sum of the two intensities is conserved due to the energy conversion. More insight can be found in the average energy-transfer rate $\eta = (I'_{1 \max} - I'_{1 \min}) / (I'_1 + I'_2)$ with various input intensities shown in Fig. 2(c), which can indicate the average energy transfer between two waves despite their relative phases. Here, η reaches its maximum around 0.92 with the initial intensities' ratio

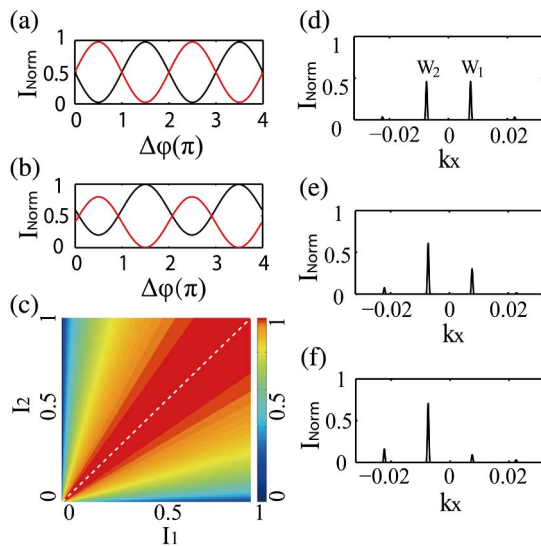


Fig. 2. Theoretical results of the TWM process. (a) Intensities of the output waves, I'_1 and I'_2 , with normalized initial intensities, I_1 and I_2 , are 0.5, 0.5, oscillate with a period of 2π when varying the phase difference $\Delta\varphi$ linearly, but with a π phase jump to each other. The average energy transfer rate η is 0.92. Black (red) curve represents I'_1 (I'_2). (b) When the initial intensities (I_1 , I_2) change to (0.25, 0.75), the average energy transfer rate η decreases to 0.79. (c) Average energy transfer rate η vary with the initial intensities, I_1 , I_2 , η reaches its maximum value as 0.92 when $I_1 = I_2$. (d)–(f) Spatial Fourier analysis of the TWM process is shown in the vector K -space as the phase difference $\Delta\varphi$ are 0, $\pi/6$, $\pi/2$, respectively, where the initial intensities (I_1 , I_2) are (0.5, 0.5). With the phase varying of $\Delta\varphi$ from 0 to $\pi/2$, the energy of W_1 transfer into W_2 gradually, which verifies the validity of (a).

equals to 1 while it decreases to zero when only one beam is present. Physically, this phenomenon is related to the balanced or unbalanced interferences, which we shall explain later.

More insight can be seen in the spatial Fourier spectrum in Figs. 2(d)–2(f), which is obtained by the spatial domain Fourier analysis using a beam propagation method [24] assuming quasi-static approximation. With equal input intensities but a frequency difference of the acoustic frequency of the AOM, the two waves are incident on the AOM at $\pm\theta_B$ positive and negative Bragg degree, corresponding to two sites along the k_x axis around $\pm 7.45 \times 10^{-3}$ rad in Fig. 2(d). The two waves apparently do not mix with each other with zero phase delay, thus evolving into two equal-intensity peaks at the output face of AOM in Fig. 2(d). However, when varying $\Delta\varphi$ from 0 to $\pi/2$, one wave at $+\theta_B$ grows while sucking the energy from the other one at $-\theta_B$. More interestingly, such process seems to be cascaded, giving rise to a third wave at $-1.5\theta_B$, effectively forming the Raman–Nath diffraction [25].

3. TWO-WAVE MIXING IN THE MOVING GRATING

Figure 3 shows the schematic of our experiment: a He–Ne laser with wavelength $\lambda = 632.8$ nm and frequency ω_1 enters an AOM driven by frequency $\Omega = 100$ MHz at the first positive Bragg angle of 0.426° ; as a result, a second wave with frequency of $\omega_2 = \omega_1 + \Omega$ can be generated at the first negative Bragg angle, thus fulfilling the phase-matching condition $k_2 = k_1 + K$ in Fig. 1(c). The AOC involved in this paper is a TeO_2 crystal with a height of $H = 2$ mm and a length of $L = 16$ mm. A longitudinal acoustic wave mode along the negative x direction has a corresponding velocity $V = 4260$ m/s. The effective component of the strain field is $S_3 = \sqrt{2I_a / (\rho V^3)}$ and the photoelastic constant is $p_{13} = 0.34$ [26], where $\rho = 5990$ kg/m³ is the density of the crystal and I_a is the intensity of the acoustic in the AOC. The acoustic wave applied on the crystal is generated by a power of $P = 0.3$ W with a frequency of $f = 100$ MHz, so the value of intensity $I_a = P / HL$ is 0.94 W/cm² and $\kappa = 0.62$ cm⁻¹. In this manner, two waves with the exact frequency difference of the acoustic wave are created as the inputs; later, they can be rerouted back into the same AOM at the first positive and negative Bragg angles through a set of mirrors (M1: M4) to conduct the TWM experiment. The input power of the He–Ne laser is 2 mW. Note that the position of the two waves has been interchanged in order to fulfill the phase matching condition in a backward way. We carefully vary their intensity ratio at the incident point B by an attenuator and control their phase difference by rotating a thin glass slice. With the same input intensities, two waves' intensities indeed oscillate sinusoidally in the experiment [Figs. 3(b) and 3(c)], which is similar to theoretical results in Fig. 2. Physically, this can be interpreted as the interference between the two waves: taking the beam path M2-B-P2, for example, the incident beam M2-B is at frequency $\omega_2 = \omega_1 + \Omega$, the Bragg scattered beam B-P2 gains a frequency upshifting by Ω off the incident beam M3-B at frequency ω_1 , resulting in interference along the beam path B-P2. Meanwhile, similar interference occurs between the incident beam M3-B-P1 and the beam B-P1, which is scattered off the beam M2-B-P2. Hence,

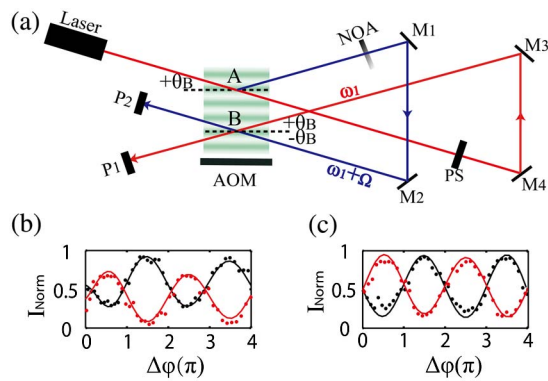


Fig. 3. Schematic of the experimental setup for TWM and the experimental measurements. (a) Zero/first order Bragg diffraction beam with frequency $\omega_1/\omega_1 + \Omega$ occurring at point A is reflected by M4-M3/M1-M2 back into the AOM at $+\theta_B/-\theta_B$ at point B, where TWM undergoes in the refractive index moving grating induced by acoustic waves. (b) and (c) Experimental measurement (dot) of the intensity oscillations during the phase varying and the corresponding fitted curves (solid). Black (red) dots represent I'_1 (I'_2). Energy transfer depends on the phase difference $\Delta\phi$ during the TWM and the ratios of I_1 and I_2 . (b) Energy transfer rate η reaches 0.68 for initial intensities (0.25, 0.75) in (b), and 0.8 for initial intensities (0.5, 0.5) in (c). NOA, neutral optical attenuator; M1-M4, mirror; P1; 2, photodiode; AOM, acoustic optical modulator; PS, phase shifter.

the intensity spectra in Figs. 3(b) and 3(c) exhibit a phase-dependent oscillation. Furthermore, the initial intensity ratio determines the depths of oscillations along the two paths, as shown in Fig. 3. The measured average energy transfer rate η for the intensity ratios 0.5:0.5 and 0.25:0.75 are 0.68 and 0.80, respectively, which is slightly lower than the theoretical value in Fig. 2 due to the limitation of the experiments, e.g., alignment, coherence. Nevertheless, the experimental measurements here confirm the interference nature of the two-wave mixing in a moving grating.

4. COMPARISON EXPERIMENT

In order to demonstrate the unidirectional nature of TWM with respect to the propagation axis of the acoustic wave, we have conducted a set of comparison experiments. Unlike nonreciprocal TWM in nonlinear media [26], our work could be understood by considering a reciprocal scheme along the beam path C-BS-P1 [Fig. 4(b)] of the original phase matching condition for the forward two-wave mixing [Fig. 1(c)]; here, if reciprocity still holds, the wave vector K of the acoustic wave should be reversed. However, the acoustic wave driven by the AOM only propagates upward in Fig. 4(b), thus failing to satisfy the phase matching condition in this backward manner. Hence, TWM between $k_2(\omega_1 + \Omega)$ and $k_1(\omega_1)$ is forbidden, but the Bragg scattering of $k_2(\omega_1 + \Omega)$ to $k_3(\omega_1 + 2\Omega)$ is still valid in Fig. 4(c). Similar works have shown the optical isolation inside a photonic crystal fiber using SBS [19] and optical isolation by dynamic modulation [20,27], both of which rely on the unidirectional moving grating induced either by acoustic wave or external modulation. Experimentally, we configure a setup by directly reflecting two waves at the first positive

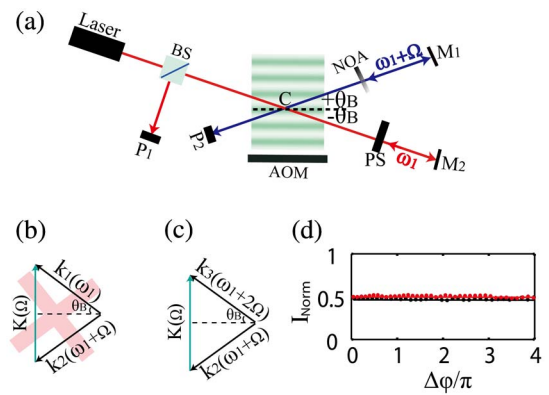


Fig. 4. Schematic of the comparison experiment for unidirectional TWM. (a) Zero/first order Bragg diffraction beam with frequency $\omega_1/\omega_1 + \Omega$ occurred at point A is reflected by M2/M1 back into the AOM at $-\theta_B/+\theta_B$ at point B. However, the phase matching condition is no longer valid in such backward manner, as shown in (b), while the Bragg scattering condition is fulfilled in (c). (d) Measured intensities I'_1 and I'_2 in with phase varying indicate no TWM occurs in the reversed scheme.

and negative Bragg angle in Fig. 4 without interchanging their positions as in Fig. 3, thus mimicking the reversed configuration of TWM in Fig. 3. For now, TWM no longer occurs, no matter how the relative phase is varying or what their initial intensity ratios are. Physically, this is because the interference effect mentioned above is inhibited; for example, along the beam path C-BS-P1, the reflected wave along M1-C with frequency $\omega_2 = \omega_1 + \Omega$ is once again scattered off the same moving grating, gaining another frequency upshifting by $\omega_3 = \omega_1 + 2\Omega$. This is 2Ω more than the wave reflected along M2-C-P1; no interference like the forward TWM case happens in this way.

5. DISCUSSION AND CONCLUSION

In conclusion, we would like to comment on the implied applications with this phase-controlled TWM scheme: the newly rising radio/microwave over fiber technology converts radio or microwave signals into optical modulation over an optical channel to facilitate the signals' long-distance transmission, which is favorable by many applications such as satellite communication, cable television networks, and wireless communication [28]. Here, radio/microwave frequency spacing between channels can be accessible by the current TWM for frequency conversion and signal switching/modulation purposes in a controlled manner through phase.

In summary, we demonstrate that the near-degenerated two-wave mixing effect in a moving optical grating inside an AOM is due to the interference nature between the waves. Our studies separate the physical processes of the generation of the moving grating and TWM, thus clearly showing the important role of two waves' relative phase during the energy transfer of TWM. It may offer a unique opportunity for optical information processing at a low-light level. Moreover, we also show that TWM here is unidirectional owing to the unidirectional propagation of the moving grating, which can provide a new avenue for applications such as in optical isolation in the near future.

Funding. National 1000-plan Program (Youth); National Natural Science Foundation of China (NSFC) (11304201, 61475100); Shanghai Scientific Innovation Program (14JC1402900).

REFERENCES

1. P. Yeh, "Two-wave mixing in nonlinear media," *IEEE J. Quantum Electron.* **25**, 484–519 (1989).
2. J.-P. Huignard and A. Marrakchi, "Two-wave mixing and energy transfer in $\text{Bi}_{12}\text{SiO}_{20}$ crystals: application to image amplification and vibration analysis," *Opt. Lett.* **6**, 622–624 (1981).
3. J. Huignard and A. Marrakchi, "Coherent signal beam amplification in two-wave mixing experiments with photorefractive $\text{Bi}_{12}\text{SiO}_{20}$ crystals," *Opt. Commun.* **38**, 249–254 (1981).
4. J. Cao, Y. Zheng, Y. Feng, X. Chen, and W. Wan, "Metal-free flat lens using negative refraction by nonlinear four-wave mixing," *Phys. Rev. Lett.* **113**, 217401 (2014).
5. Y. Zheng, H. Ren, W. Wan, and X. Chen, "Time-reversed wave mixing in nonlinear optics," *Sci. Rep.* **3**, 3245 (2013).
6. H. Kogelnik, "Coupled wave theory for thick hologram gratings," *Bell Syst. Tech. J.* **48**, 2909–2947 (1969).
7. A. Yariv and P. Yeh, *Optical Waves in Crystals* (Wiley, 1984).
8. P. Yeh, *Introduction to Photorefractive Nonlinear Optics* (Wiley, 1993).
9. A. Yariv and D. M. Pepper, "Amplified reflection, phase conjugation, and oscillation in degenerate four-wave mixing," *Opt. Lett.* **1**, 16–18 (1977).
10. N. K. Efremidis, J. Hudock, D. N. Christodoulides, J. W. Fleischer, O. Cohen, and M. Segev, "Two-dimensional optical lattice solitons," *Phys. Rev. Lett.* **91**, 213906 (2003).
11. J. W. Fleischer, M. Segev, N. K. Efremidis, and D. N. Christodoulides, "Observation of two-dimensional discrete solitons in optically induced nonlinear photonic lattices," *Nature* **422**, 147–150 (2003).
12. W. Wan, S. Jia, and J. W. Fleischer, "Dispersive superfluid-like shock waves in nonlinear optics," *Nat. Phys.* **3**, 46–51 (2007).
13. S. Jia, W. Wan, and J. W. Fleischer, "Dispersive shock waves in nonlinear arrays," *Phys. Rev. Lett.* **99**, 223901 (2007).
14. C. E. Rüter, K. G. Makris, R. El-Ganainy, D. N. Christodoulides, M. Segev, and D. Kip, "Observation of parity-time symmetry in optics," *Nat. Phys.* **6**, 192–195 (2010).
15. H. J. Eichler, P. Günter, and D. W. Pohl, *Laser-Induced Dynamic Gratings* (Springer, 1986).
16. R. Chiao, C. Townes, and B. Stoicheff, "Stimulated Brillouin scattering and coherent generation of intense hypersonic waves," *Phys. Rev. Lett.* **12**, 592–595 (1964).
17. J. J. Ottusch and D. A. Rockwell, "Stimulated Brillouin scattering phase-conjugation fidelity fluctuations," *Opt. Lett.* **16**, 369–371 (1991).
18. R. W. Boyd, *Nonlinear Optics* (Academic, 2003).
19. M. Kang, A. Butsch, and P. S. J. Russell, "Reconfigurable light-driven opto-acoustic isolators in photonic crystal fibre," *Nat. Photonics* **5**, 549–553 (2011).
20. Z. Yu and S. Fan, "Complete optical isolation created by indirect inter-band photonic transitions," *Nat. Photonics* **3**, 91–94 (2009).
21. B. Peng, F. Chen, Y. Tan, and D. Kip, "Two-wave mixing of ion-implanted photorefractive waveguides in near-stoichiometric Fe:LiNbO_3 crystals," *Opt. Mater.* **33**, 773–776 (2011).
22. S. Balasubramanian, I. Lahiri, Y. Ding, M. Melloch, and D. Nolte, "Two-wave-mixing dynamics and nonlinear hot-electron transport in transverse-geometry photorefractive quantum wells studied by moving gratings," *Appl. Phys. B* **68**, 863–869 (1999).
23. G. C. Valley, "Two-wave mixing with an applied field and a moving grating," *J. Opt. Soc. B* **1**, 868–873 (1984).
24. J. Van Roey, J. Van der Donk, and P. Lagasse, "Beam-propagation method: analysis and assessment," *J. Opt. Soc. B* **71**, 803–810 (1981).
25. M. G. Moharam and L. Young, "Criterion for Bragg and Raman-Nath diffraction regimes," *Appl. Opt.* **17**, 1757–1759 (1978).
26. N. Uchida and Y. Ohmachi, "Elastic and photoelastic properties of TeO_2 single crystal," *J. Appl. Phys.* **40**, 4692–4695 (1969).
27. M. Zha and P. Günter, "Nonreciprocal optical transmission through photorefractive $\text{KNbO}_3:\text{Mn}$," *Opt. Lett.* **10**, 184–186 (1985).
28. H. Al-Raweshidy and S. Komak, *Radio Over Fiber Technologies for Mobile Communications Networks* (Artech House, 2002).